

Genetically engineered immunoglobulins reveal structural features controlling segmental flexibility

(hinge dynamics/antibody isotypes/nanosecond fluorescence polarization/dansyl hapten)

WILLIAM P. SCHNEIDER*^{†‡}, THEODORE G. WENSEL[§], LUBERT STRYER[§], AND VERNON T. OI[†]

*Department of Biological Sciences, Stanford University, Stanford, CA 94305; [†]Becton Dickinson Immunocytometry Systems, 2375 Garcia Avenue, Mountain View, CA 94043; and [§]Department of Cell Biology, Stanford University School of Medicine, Stanford, CA 94305

Contributed by Lubert Stryer, December 10, 1987

ABSTRACT We have carried out nanosecond fluorescence polarization studies of genetically engineered immunoglobulins to determine the structural features controlling their segmental flexibility. The proteins studied were hybrids of a relatively rigid isotype (mouse IgG1) and a relatively flexible one (mouse IgG2a). They have identical light chains and heavy chain variable regions and have the same combining sites for ϵ -dansyl-L-lysine, a fluorescent hapten. The fluorescence of the bound dansyl chromophore was excited at 348 nm with subnanosecond laser pulses, and the emission in the nanosecond time range was measured with a single-photon-counting apparatus. The emission anisotropy kinetics of the hybrid antibodies revealed that segmental flexibility is controlled by the heavy chain constant region 1 (C_{H1}) as well as by the hinge. In contrast, the C_{H2} and C_{H3} domains did not influence segmental flexibility. The hinge and C_{H1} domains must be properly matched to allow facile movement of the Fab units. Studies of hybrids of IgG1 and IgG2a within C_{H1} showed that the loop formed by residues 131-139 is important in controlling segmental flexibility. X-ray crystallographic studies by others of human IgG1 have shown that this loop makes several van der Waals contacts with the hinge.

The Fab units of immunoglobulins have considerable rotational freedom about the hinge joining them to the Fc unit (1-4). This mobility of domains, termed segmental flexibility, enhances the binding of antibodies to multivalent antigens; the distance between combining sites and their angular relationship can be adjusted to match the pattern of antigenic determinants (1, 5, 6). Segmental flexibility may also be important for effector functions such as complement fixation (7, 8). A strong correlation between flexibility and complement-fixation activity has been found in a series of 10 mouse, human, and rabbit immunoglobulin isotypes (9, 10). The biological significance of segmental flexibility extends beyond immunoglobulins. The rotational motion of domains is also important for the function of many other proteins, as exemplified by myosin, spectrin, hexokinase, and viral coat proteins (11).

How is segmental flexibility controlled? We have explored this question by studying the rotational dynamics of hybrid anti-dansyl antibodies derived from two mouse isotypes, the relatively rigid IgG1 and the relatively flexible IgG2a. The amino acid sequences of the heavy chain constant regions (C_H) of IgG1 and IgG2a are 85% identical in C_{H1} , 31% in the hinge, 66% in C_{H2} , and 63% in C_{H3} (12). In addition to displaying different degrees of segmental flexibility, IgG1 and IgG2a differ markedly in effector functions, such as antigen-directed cell-mediated cytotoxicity (ADCC; ref. 13), complement fixation (14), and Fc receptor binding (for a review, see ref. 15). The hybrid antibodies studied here all

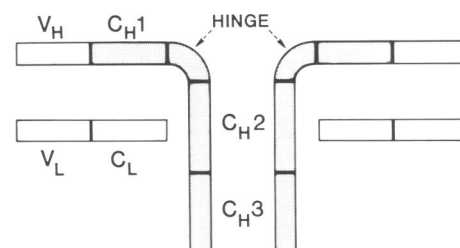


FIG. 1. Schematic diagram of IgG structure. The antigen-binding sites are formed by heavy and light chain variable regions, V_H and V_L . Isotypes differ in the constant region of the heavy chain (C_{H1} , hinge, C_{H2} , and C_{H3}), which is shaded. The genetically engineered antibodies studied here are hybrids of IgG1 and IgG2a, which differ in the shaded regions. The unshaded regions are the same in all the antibodies of this study.

have the same light chains and heavy chain variable regions, which give them identical anti-dansyl combining sites (Fig. 1). Their heavy chains have portions of the sequence of one isotype replaced by the corresponding region of the other isotype. The compositions of the hybrid antibodies are given in Table 1.

The segmental flexibility of the hybrid antibodies was determined by measuring their fluorescence polarization kinetics in the nanosecond time range. A solution of antibody containing bound ϵ -dansyl-L-lysine was excited by a subnanosecond pulse of vertically polarized light to create an ensemble of chromophores preferentially aligned in the vertical direction. The orientations of these excited chromophores then become randomized by rotational Brownian motion, which depends both on the global rotation of the antibody and on its internal modes of flexibility. These motions can be monitored by measuring the intensities of the vertically polarized [$F_y(t)$] and horizontally polarized [$F_x(t)$] components of the fluorescence emission as a function of time following the excitation pulse. The emission anisotropy $A(t)$ is defined as:

$$A(t) = \frac{F_y(t) - F_x(t)}{F_y(t) + 2F_x(t)} \quad [1]$$

The emission anisotropy kinetics of the hybrid antibodies identified the regions of the immunoglobulin molecule that are critical in controlling segmental flexibility.

MATERIALS AND METHODS

Preparation of Hybrid Antibodies. The 11 proteins listed in Table 1 are anti-dansyl IgGs with identical light chains and

Table 1. Domain structure and segmental flexibility of genetically engineered antibodies used in this study

Protein	C _H 1*			C _H 2	C _H 3	$\langle\phi\rangle$ with or without dithiothreitol, ns	
	N term.	C term.	Hinge			Without	With
Interdomain hybrids							
IgG1	γ 1	γ 1	γ 1	γ 1	γ 1	83	71
IgG2a	γ 2a	γ 2a	γ 2a	γ 2a	γ 2a	61	49
Hingeless IgG2a	γ 2a	γ 2a	Deleted	γ 2a	γ 2a	84	87
Hybrid 2	γ 1	γ 1	γ 2a	γ 2a	γ 2a	84	55
Hybrid 3	γ 1	γ 1	γ 1	γ 2a [†]	γ 2a	82	61
Hybrid 9	γ 2a	γ 2a	γ 1	γ 1	γ 1	108	76
Hybrid 10	γ 2a	γ 2a	γ 2a	γ 1 [‡]	γ 1	62	52
Intra-C _H 1 hybrids							
Hybrid 11	γ 2a	γ 1	γ 1	γ 1	γ 1	114	60
Hybrid 12	γ 1	γ 2a	γ 2a	γ 2a	γ 2a	89	49
Hybrid 13	γ 1	γ 2a	γ 1	γ 1	γ 1	81	76
Hybrid 14	γ 2a	γ 1	γ 2a	γ 2a	γ 2a	64	47

The proteins listed are anti-dansyl IgGs with identical light chains and heavy chain variable regions. Each C_H domain (C_H1, hinge, C_H2, and C_H3) was derived either from mouse IgG1 (γ 1 heavy chain) or mouse IgG2a (γ 2a heavy chain). The crossover points in the corresponding DNA sequences were either within introns or within the coding regions at the positions coding for the amino acids as indicated in the table footnotes in the EU numbering system (24). Hybrids 2, 3, 9, and 10 correspond to proteins γ 1 γ 2a-2, -3, -9, and -10, respectively, from ref. 16. The segmental flexibility of each immunoglobulin was determined from nanosecond fluorescence anisotropy kinetics as described in the text. The mean rotational correlation time $\langle\phi\rangle$ calculated from the two exponential fit is given.

*The N-terminal (term.) half of C_H1 = amino acids 118–161; the C-terminal half = amino acids 162–215.

[†] γ 1 to residue 238; γ 2a from residue 239 on.

[‡] γ 2a to residue 238; γ 1 from residue 239 on.

heavy chain variable regions. Each C_H domain (C_H1, hinge, C_H2, and C_H3) was derived either from mouse IgG1 (γ 1 heavy chain) or mouse IgG2a (γ 2a heavy chain) or both. The preparation of the proteins with normal IgG1 and IgG2a heavy chains, hybrids 2–10, and the hingeless IgG2a has been described (16). These proteins correspond to γ 1 γ 2a8 (IgG1); γ 1 γ 2a1 (IgG2a) and γ 1 γ 2a-2, -3, -9, and -10 (hybrids 2, 3, 9 and 10, respectively); and IgG2a Δ hinge (hingeless IgG2a) described previously (16). The sequence junctions in the hybrids occur both within and between domains. The junction positions are indicated on Table 1 in the EU numbering system. C_H gene segments for hybrid proteins 11 through 14 were constructed by using the conserved *Bam*HI restriction site that occurs at codon 161 of both the IgG1 and IgG2a C_H1 coding regions. The hybrid 11 C_H gene segment was constructed by ligating a 240-base-pair (bp) *Sal* I–*Bam*HI fragment from the IgG2a C_H gene segment that encodes the N-terminal portion of the C_H1 region of γ 2a chain to a 4.6-kilobase (kb) *Bam*HI–*Sal* I fragment from the IgG1 C_H gene segment that encodes the C-terminal portion of C_H1, the hinge, C_H2, and C_H3 regions of γ 1 chain. The hybrid 14 C_H gene segment was constructed by ligating the same 240-bp IgG2a C_H gene segment to a 4.6-kb *Bam*HI–*Sal* I fragment from the hybrid 2 C_H gene segment encoding the C-terminal portion of the C_H1 region of γ 1 as well as the hinge, C_H2, and C_H3 regions of γ 2a. The hybrid 12 C_H gene segment was constructed by ligating a 240-bp *Sal* I–*Bam*HI fragment from the IgG1 C_H gene segment encoding the γ 1 N-terminal portion of the C_H1 region to a 4.6-kb *Bam*HI–*Sal* I fragment from the IgG2a C_H gene segment that encodes the C-terminal portion of C_H1, hinge, C_H2, and C_H3 regions of γ 2a. The hybrid 13 C_H gene segment was constructed by ligating the same 240-bp fragment from IgG1 C_H gene segment to a 2.3-kb *Bam*HI–*Sal* I fragment from the hybrid 9 C_H gene segment encoding the γ 2a C-terminal portion of the C_H1 region in addition to the hinge, C_H2, and C_H3 regions of γ 1. The hybrid 11 through 14 gene segments were ligated into the *Sal* I site of pMLSVgptDNS-VDJ and expressed as described (16). Reducing and nonreducing NaDod-SO₄/PAGE analyses of hybrids 11, 12, 13, and 14 gave the

same patterns as did hybrid 9, hybrid 2, IgG1, and IgG2a, respectively (16).

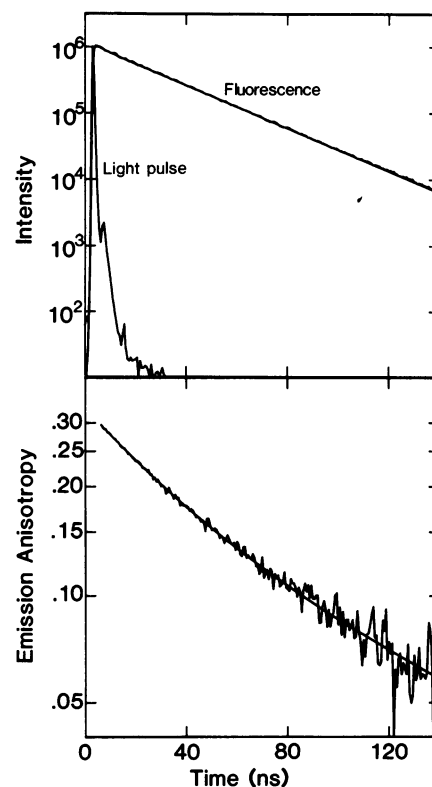


FIG. 2. Fluorescence and emission anisotropy decay data from hybrid 3, a genetically engineered anti-dansyl IgG, having IgG1-derived C_H1 and hinge domains and IgG2a-derived C_H2 and C_H3 domains. (Upper) Fluorescence decay of bound ϵ -dansyl-L-lysine and the instrument response to the light pulse. Superimposed on the fluorescence data is a smooth line corresponding to a biexponential decay with lifetimes of 26.9 ns (88%) and 3.5 ns (12%). (Lower) Time course of the emission anisotropy of this IgG. Superimposed on the data is a smooth line corresponding to a biexponential decay with rotational correlation times of $\phi_1 = 35.0$ ns ($a_1 = 0.140$) and $\phi_2 = 121.1$ ns ($a_2 = 0.171$).

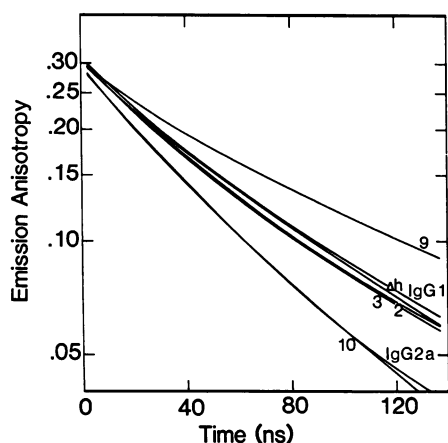


FIG. 3. Comparison of anisotropy decay kinetics displayed by parental and interdomain hybrid IgGs. The emission anisotropy decays are displayed as smooth curves representing the best fits obtained for biexponential decay functions. The numbering corresponds to the name for each protein as listed in Table 1 (e.g., 2 for hybrid 2, etc.), and Δh refers to the hingeless IgG2a.

Conditions for Fluorescence Anisotropy Measurements. Anisotropy measurements were made with antibody at 0.2 mg/ml (2.7 μ M combining sites) and 0.5 μ M hapten (ϵ -dansyl-L-lysine) in 150 μ l of 0.15 M NaCl/50 mM Tris-HCl, pH 7.8. The temperature was held at 20°C. To test for the effects of reduction, disulfide bonds were reduced by incubating the hapten/antibody solution used for anisotropy measurements with 2 mM dithiothreitol for 20 min at 23°C.

Nanosecond Instrumentation. Measurements were made with an instrument similar to one described previously (9, 17) with the following modifications (18). Picosecond pulses at 348 nm were obtained by frequency doubling the 696-nm output of the dye DCM (Exciton Chemical, Dayton, OH) in a cavity-dumped dye laser (Spectra-Physics, Mountain View, CA; models 344 and 375) dumped by a mode-locked argon-ion laser (Spectra-Physics model 171). Emitted light passed through a film polarizer, which was periodically rotated to alternate between detection of vertically (F_y) and horizontally (F_x) polarized components by the photomultiplier (Hamamatsu, Hamamatsu City, Japan; R-928). The single-photon-counting electronics used a constant-fraction discriminator (Tennelec, Oak Ridge, TN; TC 454) along with a time-to-digital converter and histogramming memory (Le-Croy, Spring Valley, NY; models 4202 and 3588) interfaced

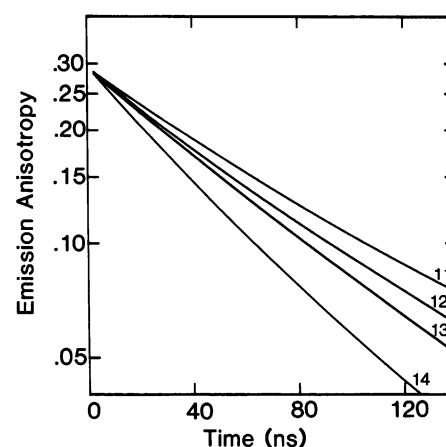


FIG. 4. Anisotropy decay kinetics of C_{H1} -loop hybrids. Data for the four immunoglobulins, hybrids 11 through 14, whose C_{H1} domains are roughly half IgG1-derived and half IgG2a-derived (Table 1) are displayed as in Fig. 3 and labeled in accordance with the names in Table 1.

with a computer (LSI 11/23, Digital Equipment, Marlboro, MA). Data sets containing 3×10^5 counts in the peak channel were obtained in 10–15 min.

The observed function $A(t)$ was fit to a sum of two exponential decays by using a nonlinear least-squares algorithm (2): $A(t) = a_1 \exp -[t/\phi_1] + a_2 \exp -[t/\phi_2]$. A mean rotational correlation time $\langle \phi \rangle = (a_1 \phi_1 + a_2 \phi_2)/(a_1 + a_2)$ can be calculated for each antibody from the two-exponential decay function fit to the data. The value of $\langle \phi \rangle$ decreases with increasing segmental flexibility. The use of this parameter facilitates comparison of the results obtained for different antibodies here and in previous work.

RESULTS

The fluorescence and emission anisotropy kinetics of a genetically engineered anti-dansyl IgG (hybrid 3) are shown in Fig. 2. The excited state lifetimes of all the immunoglobulins in this study were virtually identical. This result and the fact that their fluorescence emission spectra were indistinguishable (data not shown) provide strong evidence that the combining sites have identical three-dimensional structures in addition to identical amino acid sequences and that the different heavy chain constant domains do not influence hapten binding.

	118		161	
Mouse IgG1	P	GSAAQ N M	V	N-terminal
Mouse IgG2a	AKTTAPSVYPLAPVCGDTTGSSTLGLVKGYFPEPVTLTWNSG			portion
KOL	S KG F	SSKS S GTAA	D VS	of CH1
	162		215	
IgG1		P PR ETV		C-terminal
IgG2a	SLSSGVHTFPVAVLQS	DLTYLSSSVTVTSTWPSQSITCNVAHPASSTKVKDKKI		portion
KOL	A T	SG S V P SLGT TYI N KP N	V	of CH1
	216		230	
IgG1	V DCG	K I T		
IgG2a	EPRG PTTKPCPPCKCP			Hinge
KOL	KSCDKTHT			

FIG. 5. Comparison of amino acid sequences (in the single-letter code) of C_H domains of mouse IgG1 and IgG2a (12) and human IgG1 (Kol). The full IgG2a sequence is listed; residues of mouse IgG1 that differ are given above, and those of Kol that differ are given below. Deletions are indicated by a line. EU numbers are given above each row of the sequence. The break between the first and second row (i.e., Gly-161) corresponds to the beginning of the restriction site used to generate the inter- C_{H1} hybrid antibodies hybrid 11 through hybrid 14. The first hinge cysteine of mouse IgG1 is aligned with Cys-220 of Kol, which forms a disulfide bond to light chain Cys-213. In IgG2a, C_{H1} supplies the heavy chain's contribution (probably Cys-132) to the heavy-light disulfide bond.

In contrast, the hybrid immunoglobulins exhibited distinctive emission anisotropy decay curves. The interdomain hybrids fell into three well-defined groups with respect to flexibility (Fig. 3). Two molecules, IgG2a ($\langle\phi\rangle = 61$ ns) and hybrid 10 ($\langle\phi\rangle = 62$ ns), had segmental flexibility like that of the flexible IgG2a isotype. The largest group includes IgG1 ($\langle\phi\rangle = 83$ ns), hybrid 2 ($\langle\phi\rangle = 84$ ns), hingeless IgG2a ($\langle\phi\rangle = 84$ ns), and hybrid 3 ($\langle\phi\rangle = 82$ ns), whose segmental flexibility was essentially the same as that of the more rigid parental isotype, IgG1. Hybrid 9 ($\langle\phi\rangle = 108$ ns) was unique in being significantly more rigid than either parental molecule.

Hybrids within the C_H1 domain also displayed a range of flexibility behavior (Fig. 4). Hybrid 14 ($\langle\phi\rangle = 64$ ns) displayed the segmental flexibility characteristic of IgG2a, and hybrid 13 ($\langle\phi\rangle = 81$ ns) behaved like IgG1. Hybrid 12 ($\langle\phi\rangle = 89$ ns) was slightly more rigid than IgG1, while hybrid 11 ($\langle\phi\rangle = 114$ ns) was similar to hybrid 9 in being considerably more rigid than either IgG1 or IgG2a.

Regions important for flexibility can be identified by comparing the amino acid sequences of molecules differing in flexibility. Hybrid 10 has C_H2 and C_H3 sequences that are derived from the more rigid IgG1, yet it was just as flexible as IgG2a. Three molecules—hybrid 2, hingeless IgG2a, and hybrid 3—have C_H2 and C_H3 sequences derived from the more flexible IgG2a, and yet they were just as rigid as IgG1. Hence, the C_H2 and C_H3 domains do not appear to influence segmental flexibility.

The hinge region, in contrast, is clearly important in determining flexibility, as was proposed earlier (2, 3, 10, 19, 20). The two flexible molecules, IgG2a and hybrid 10, each have an IgG2a hinge, while each hybrid with an IgG1 hinge (i.e., hybrids 3 and 9) was at least as rigid as IgG1. Moreover, the hingeless IgG2a, whose entire sequence was derived from the flexible IgG2a, was as rigid as IgG1.

It is also clear that the hinge is not the only region that determines flexibility; C_H1 plays an important role as well. Hybrid 10, which was as flexible as IgG2a, has an IgG2a-

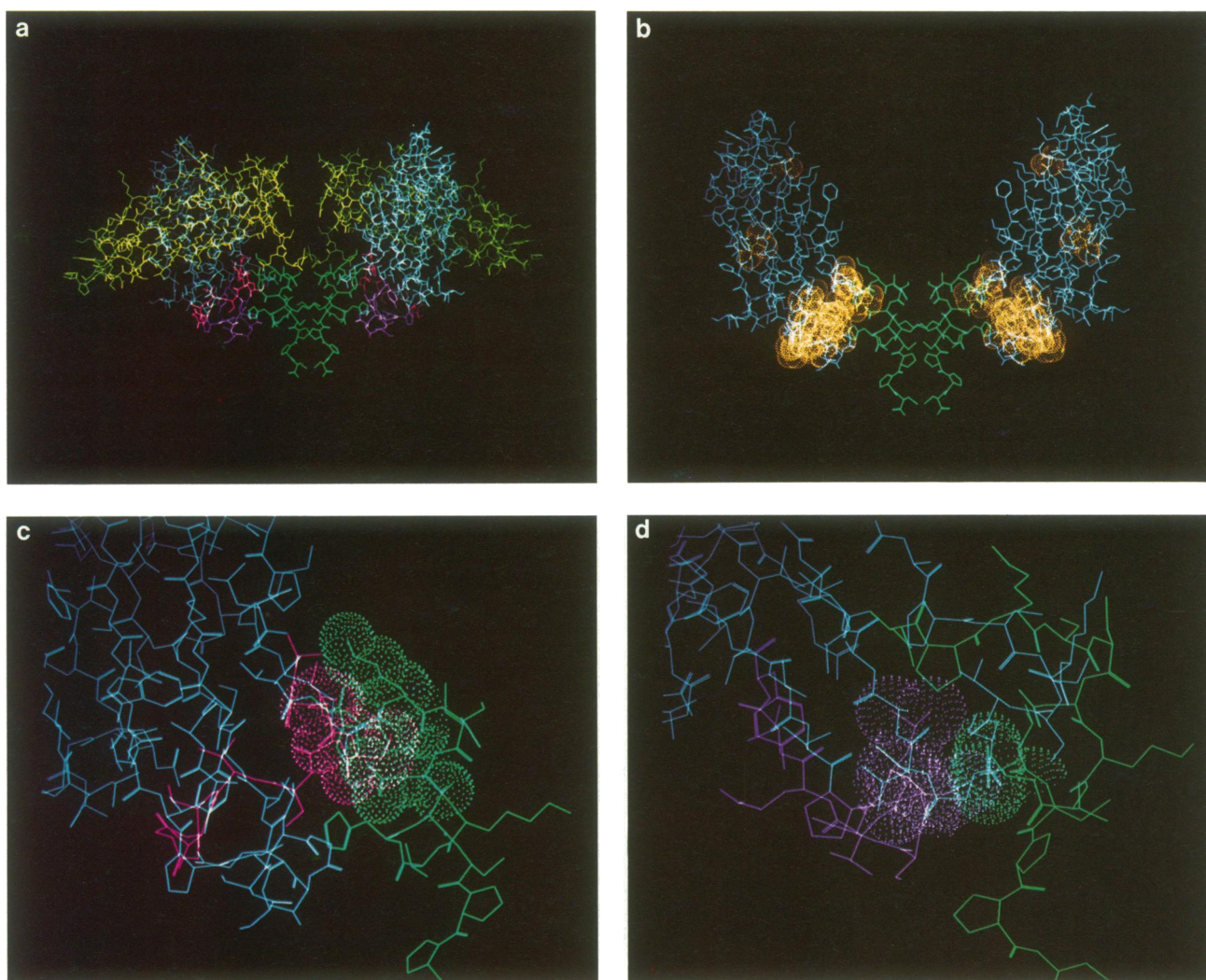


FIG. 6. Interactions between the C_H1 domain and the hinge. The drawings are based on the coordinates for the human IgG Kol reported by Marquart *et al.* (21) and were generated with the Evans and Sutherland Molecular Graphics System using the program MOGLI. (a) View of C_H1, light chain C region and hinge portions. Both symmetry-related halves are shown, with the light chain in yellow, and C_H1 in white. The hinge residues 216–230 are shown in green. (b) View of C_H1 and hinge domains showing the location of sites corresponding to sequence differences between mouse IgG1 and IgG2a in C_H1. van der Waals surfaces have been drawn in orange for the residues occupying those positions in the linear sequence at which mouse IgG1 and IgG2a differ. The hinge is in green. (c) Interactions between the 131 loop (residues 129–139, in red) of C_H1 and the hinge (green). van der Waals surfaces are drawn for the residues of C_H1 (Ser-131 and Ser-132) and the hinge (Lys-218 and Asp-221) that are in atomic contact (center–center distance of 0.4 nm or less). (d) Interactions between the 189 loop (residues 189–190, purple) and the hinge (green). van der Waals surfaces are drawn for the residues of C_H1 (Ser-190, Leu-193, and Gly-194) and the hinge (His-224) that are in atomic contact.

derived C_H1 as well as hinge. Hybrid 2, which has a hinge region derived from the flexible IgG2a but an IgG1-derived C_H1, was just as rigid as IgG1. Moreover, the one molecule (hybrid 9) that was significantly more rigid than IgG1 has an IgG1-derived hinge, but an IgG2a-derived C_H1. These results indicate that there is an interplay between C_H1 and the hinge that limits flexibility when the sequences are mismatched; that is, when C_H1 and the hinge have sequences from different parent molecules.

DISCUSSION

Correlation with Three-Dimensional Structure. The role of C_H1 in determining flexibility is particularly interesting in light of the high degree of sequence homology between C_H1 of IgG1 and IgG2a. There are only 15 amino acid differences between the two isotypes in this domain (Fig. 5), with 13 of them occurring in two clusters. There are 7 differences in the sequence 131–139 (EU numbering; ref. 24), and 6 more are found in residues 189–198. It is informative to examine the location of these regions in an immunoglobulin in which the structure of C_H1 and the adjacent hinge are known at atomic resolution by x-ray analysis. Such a molecule is the human IgG1 Kol (21), whose structure has been solved by Deisenhofer, Huber, and coworkers. The C_H1 amino acid sequence of Kol is 64% identical to mouse IgG1 and 62% identical to mouse IgG2a (Fig. 5). It seems likely that the overall folding of the polypeptide chain is similar in the mouse and human IgGs.

In the Kol structure (Fig. 6), amino acids 131–139 and 189–198 (EU numbering) are found within loops that are very near the hinge (Fig. 6*b*). We refer to these as the 131 loop and the 189 loop, respectively. All of the atoms in C_H1 that are within 0.5 nm of the hinge occur within these two loops (Ala-129, Pro-130, Ser-131, Ser-132, Ser-190, Ser-191, Leu-193, and Gly-194) or are next to the hinge in the linear sequence (Lys-214 and Val-215, corresponding to Lys-214 and Ile-215 in both mouse isotypes). Residues Gly-122 and Val-156 of Kol, which correspond to the other two sites of amino acid difference between mouse IgG2a and IgG1, are more than 1 nm distant from the hinge (Fig. 6*b*). Steric interactions between the hinge and nearby residues in C_H1 (Fig. 6) are probably responsible for the observed influence of C_H1 on flexibility.

We have more precisely identified the locus of these interactions by examining hybrids within C_H1. The sequence interchanges in this series (hybrids 11–14) occur between the 131 loop and the 189 loop (Table 1 and Fig. 6). When the segmental flexibility of these constructs was examined, a striking result was observed (Fig. 5 and Table 1). Altering the heavy chain of either IgG1 or IgG2a by replacing the 131 loop and the hinge-distant residues 122 and 156 with the corresponding amino acid residues from the other isotype renders either molecule significantly more rigid. Exchanging the sequences in the 189 loop, in contrast, has virtually no effect on segmental flexibility. Thus, the importance of C_H1 to segmental flexibility can be attributed to the sequence differences in the N-terminal half of C_H1 and is probably due to interactions of the 131 loop with the hinge (Fig. 6*c*). The differences in flexibility between the hybrid immunoglobulins are not solely due to different disulfide bond patterns. These antibodies have different degrees of flexibility even after the addition of 2 mM dithiothreitol (Table 1).

Conclusions. The fluorescence depolarization kinetics of these hybrid immunoglobulins reveal clearly the regions responsible for segmental flexibility. The C_H2 and C_H3 domains of the Fc portion are not involved; rather, the characteristic flexibility of each protein is the result of an interplay between the hinge region and C_H1. This interaction has been further localized: previous work (10, 22, 23) implicated the

hinge residues on the N-terminal side of the inter-heavy-chain disulfide bonds, and the present results pinpoint the hinge proximal-loop formed by residues 131–139 in C_H1.

As noted above, a number of functional correlations have been suggested between segmental flexibility and immunoglobulin function. The present work, which defines the structural features governing flexibility, makes it possible to begin separating the effects of segmental flexibility from effects due to regions of amino acid sequence that form specific recognition sites for proteins mediating effector functions. For example, single amino acid substitutions in C_H1 could dramatically alter flexibility without directly perturbing recognition sites of C_H2 and C_H3. The effects of such changes on complement activation and Fc receptor binding would clearly define the role of flexibility in these functions. Work of this kind may eventually make possible the precise engineering of antibodies with predictable dynamic properties and effector-triggering capabilities as well as antigen-recognition specificities.

We thank Dr. Charles Yanofsky, in whose laboratory the construction of the proteins used in these experiments was initiated, and Dr. T. Minh Vuong for his work in constructing the instrument used for the emission anisotropy measurements. This work was supported by a National Institutes of Health grant (GM24032) to L.S. and a National Research Service Award (EY05815) to T.G.W.

1. Valentine, R. C. & Green, N. M. (1967) *J. Mol. Biol.* **27**, 615–617.
2. Yguerabide, J., Epstein, H. F. & Stryer, L. (1970) *J. Mol. Biol.* **51**, 573–590.
3. Cathou, R. E. (1978) *Compr. Immunol.* **5**, 37–83.
4. Hanson, D. C., Yguerabide, J. & Schumaker, V. N. (1985) *Mol. Immunol.* **22**, 237–244.
5. Romans, D. G., Tilley, C. A., Crookston, M. C., Falk, R. E. & Dorrington, K. J. (1977) *Proc. Natl. Acad. Sci. USA* **74**, 2531–2535.
6. Jackson, A. P., Siddle, K. & Thompson, R. J. (1983) *Biochem. J.* **215**, 505–512.
7. Feinstein, A., Richardson, N. & Taussig, M. J. (1986) *Immunol. Today* **7**, 169–174.
8. Dorrington, K. J. & Klein, M. H. (1982) *Mol. Immunol.* **19**, 1215–1221.
9. Oi, V. T., Vuong, T. M., Hardy, R., Reidler, J., Dangel, J., Herzenberg, L. A. & Stryer, L. (1984) *Nature (London)* **307**, 136–140.
10. Dangel, J. L. (1986) Thesis (Stanford Univ., Stanford, CA).
11. Bennett, W. S. & Huber, R. (1984) *CRC Crit. Rev. Biochem.* **15**, 291–384.
12. Yamawaki-Kataoka, Y., Miyata, T. & Honjo, T. (1981) *Nucleic Acids Res.* **9**, 1365–1381.
13. Kipps, T. J., Parham, P., Punt, J. & Herzenberg, L. A. (1985) *J. Exp. Med.* **161**, 1–17.
14. Neuberger, M. S. & Rajewsky, K. (1981) *Eur. J. Immunol.* **11**, 1012–1016.
15. Burton, D. R. (1985) *Mol. Immunol.* **22**, 161–206.
16. Schneider, W. P., Oi, V. T. & Yanofsky, C. (1987) *Proteins* **2**, 81–89.
17. Reidler, J., Oi, V. T., Carlsen, W., Vuong, T. M., Pecht, I., Herzenberg, L. A. & Stryer, L. (1982) *J. Mol. Biol.* **158**, 739–746.
18. Wensel, T. G., Schneider, W. P., Oi, V. T. & Stryer, L. (1988) *SPIE Proc.*, in press.
19. Klein, M., Haeflner-Cavallion, N., Isenman, D. E., Rivat, C., Navia, M. A., Davies, D. R. & Dorrington, K. J. (1981) *Proc. Natl. Acad. Sci. USA* **78**, 524–528.
20. Beale, D. & Feinstein, A. (1976) *Q. Rev. Biophys.* **9**, 135–180.
21. Marquart, M., Deisenhofer, J., Huber, R. & Palm, W. (1980) *J. Mol. Biol.* **141**, 369–392.
22. Ito, W. & Arata, Y. (1985) *Biochemistry* **24**, 6467–6474.
23. Endo, S. & Arata, Y. (1985) *Biochemistry* **24**, 1561–1568.
24. Kabat, E. A., Wu, T. T., Reid-Miller, M., Perry, H. M. & Gottesman, K. S., eds. (1987) *Sequences of Proteins of Immunological Interest* (National Institutes of Health, Bethesda MD), 4th Ed., pp. 293–322.